

Inside a duck-billed dinosaur: Vertebral bone microstructure of *Huallasaurus* (Hadrosauridae), Upper Cretaceous of Patagonia

Tito Aureliano^{1,2}  | Aline M. Ghilardi²  | Jonatan Kaluza³  | Agustín G. Martinelli⁴ 

¹Department of Biological Chemistry,
Programa de Pós-Graduação em
Diversidade Biológica e Recursos
Naturais, Regional University of Cariri
(URCA), Crato, Brazil

²Diversity, Ichnology and Osteohistology
Research Group (DINOLab), Federal
University of Rio Grande do Norte
(UFRN), Natal, Brazil

³Fundación de Historia Natural “Félix de
Azara”, Universidad Maimónides/
CONICET, Ciudad Autónoma de Buenos
Aires, Argentina

⁴Sección Paleontología de Vertebrados,
Museo Argentino de Ciencias Naturales
“Bernardino Rivadavia”-CONICET,
Ciudad Autónoma de Buenos Aires,
Argentina

Correspondence

Tito Aureliano, Department of Biological
Chemistry, Programa de Pós-Graduação
em Diversidade Biológica e Recursos
Naturais, Regional University of Cariri
(URCA), Crato, Brazil.

Email: aureliano.tito@gmail.com

Funding information

Consejo Nacional de Investigaciones
Científicas y Técnicas; Fundação Norte-
Rio-Grandense de Pesquisa e Cultura,
Grant/Award Number: FUNPEC-UFRN/
PIB21712-2023; Fundação Cearense de
Apóio ao Desenvolvimento Científico e
Tecnológico, Grant/Award Number:
FUNCAP/FPD-0213-00295.01.01/23

Abstract

Dinosaurs evolved a unique respiratory system with air sacs that contributed to their evolutionary success. Postcranial skeletal pneumaticity (PSP) has been used to infer the presence of air sac systems in some fossil archosaurs. While unambiguous evidence of PSP is well documented in pterosaurs and post-Carnian saurischians, it remains absent within Ornithischia, challenging phylogenetic predictions. We used computed tomography to examine the internal vertebral microanatomy of three *Huallasaurus australis* specimens, a saurolophine hadrosaur from the Late Cretaceous of Patagonia, Argentina. The internal structure reveals a relatively dense trabecular architecture lacking evidence of invasive pneumaticity across the centra, neural arches, and neural spines, contrasting with the condition in post-Carnian saurischians. The internal vertebral pattern of *Huallasaurus* resembles that of silesaurs more than other apneumatic archosauriforms. These observations are consistent with the hypothesis that invasive air sac diverticula did not evolve in Ornithischia and align with the previously proposed “pelvic bellows” ventilation model for the group. The internal vertebral architecture in this hadrosaur shows superficial similarities to the trabecular structure seen in some large mammals, although functional equivalence remains speculative. The absence of invasive air sacs in *Huallasaurus*, combined with dense trabecular matrix and thin cortical walls, may have supported large body sizes or accommodated intraosseous fat reserves, though this requires further testing. This stock of fatty tissues could have provided energy for these hadrosaurs during regional migration, as observed in modern migratory mammals.

KEY WORDS

CT scan, microanatomy, morphology, Ornithischia, respiratory system

1 | INTRODUCTION

Dinosaurs represent a successful group that survived for over 233 million years. Air sac evolution may have contributed to their success by enhancing ventilation, reducing body density, and possibly aiding thermoregulation in larger organisms (Brocklehurst et al., 2020; Maina, 2006; Perry et al., 2009; Wedel, 2009). Macroscopic traces of these invasive respiratory tissues are primarily identified through postcranial skeletal pneumaticity (PSP), characterized by well-defined laminae and deep fossae (foramina) connected with internal pneumatic chambers (Britt, 1993; O'Connor, 2006; Wedel et al., 2000). Notably, unambiguous PSP evidence in dinosaurs remains limited to post-Carnian saurischians (Aureliano et al., 2023, 2024; Butler et al., 2012; Cerda et al., 2012; Forster et al., 2020; Schachner et al., 2009; Smith et al., 2021; Watanabe et al., 2015; Wedel, 2003; Windholz et al., 2020; Zurriaguz, 2024), while it appears absent in ornithischians. The absence of PSP in the earliest saurischians (Aureliano et al., 2022) and its presence in pterosaurs (Butler et al., 2009) implies that the evolution of PSP occurred independently at least three times: in sauropodomorphs, theropods, and pterosaurs. Ornithischians, however, remain outliers among ornithodirans due to their lack of PSP, contradicting parsimonious inferences predicting the presence of air sacs based on phylogenetic bracketing (Butler et al., 2012). Modifications in the thoracic and pelvic regions in ornithischians, plus the presence of gastralia early on in the evolution of the clade, are other morphological adaptations suggesting a unique “pelvic bellows” ventilation system in this group (Radermacher et al., 2021). Here we describe the internal vertebral microanatomy of three individuals of *Huallasaurus australis* (Bonaparte et al., 1984; Rozadilla et al., 2022), a saurolophine hadrosaur from the Upper Cretaceous of Northern Patagonia, Argentina. Our CT scan analysis reveals a distinctive internal architecture of the axial skeleton that differs markedly from the pneumatized condition seen in saurischians. These findings offer novel insights into the evolution of skeletal and possibly respiratory adaptations in *Huallasaurus*, with broader implications for understanding the unique functional morphology of ornithischian dinosaurs.

2 | MATERIALS AND METHODS

Institutional abbreviations: AM, Albany Museum, Makanda, South Africa; CAPPA/UFSM, Centro de Apoio à Pesquisa Paleontológica da Quarta Colônia, Universidade Federal de Santa Maria, São João do Polêsine, Rio Grande do Sul, Brazil; CEM, Laboratório de Ecologia, Federal University of Paraná, campus Pontal do Paraná,

Brazil; MACN-Pv, Museo Argentino de Ciencias Naturales “Bernardino Rivadavia”, Colección Nacional de Paleovertebrados, Buenos Aires, Argentina; NHMUK, Natural History Museum, London, UK; SAM, Iziko South African Museum, Cape Town, South Africa.

2.1 | Specimens

We analyzed three specimens referable to *H. australis* (Rozadilla et al., 2022). The selected elements of MACN-Pv RN02 include two cervical, one anterior dorsal, and one anterior caudal vertebra. The selected element of MACN-Pv RN146 comprises one posterior dorsal vertebra. The selected elements of MACN-Pv RN826 include one cervical, one anterior dorsal vertebra, and two posterior dorsal vertebrae. MACN-Pv RN02 has been designated the holotype of “*Kritosaurus*” *australis* (Bonaparte et al., 1984) was described in later contributions (Bonaparte & Rougier, 1987). Subsequently, the species was designated part of the genus *Secernosaurus*, as *S. australis* (Prieto-Marquez & Salinas, 2010). The review of all specimens from the Los Alamitos Formation permitted the proposal of a new genus, *H. australis*, with topologies recovering this taxon within saurolophine hadrosaurids, within the Kritosaurini tribe (Rozadilla et al., 2022).

2.2 | Remarks on ontogeny

The neurocentral suture is completely fused in all specimens, suggesting at least moderate ontogenetic maturity in all individuals (Brochu, 1996; Hone et al., 2016). However, the three specimens differ in size. MACN-Pv RN146 is considerably smaller than MACN-Pv RN02, and the latter is smaller than MACN-Pv RN826. Therefore, all specimens were likely individuals from different ontogenetic stages.

2.3 | Locality and horizon

The specimens came from the Upper Cretaceous (Campanian-Maastrichtian) Los Alamitos Formation, North Patagonian Massif, Río Negro Province, Argentina (Bonaparte et al., 1984; Prieto-Marquez & Salinas, 2010).

2.4 | Anatomical nomenclature

We followed Wilson (1999, 2012) and Wilson et al. (2011) nomenclature for vertebral laminae and fossae. We followed

the terminology of Wedel (2003, 2007), Wedel et al. (2000), O'Connor (2006), and Aureliano et al. (2021) for the internal vertebral structures.

2.5 | Computed tomography (CT scan)

Vertebrae were scanned at Maimónides University (Buenos Aires, Argentina) using a Siemens-Somatom Perspective 128-Channel Multislice CT scanner with

0.75 mm voxel size. Acceleration voltage varied between 90 and 120 kV in a current of 367 mA. We followed Aureliano et al. (2020, 2021) to elaborate densitometry-based rainbow color ranges based on the non-dimensional Hounsfield counts (Figure 1). Our CT densitometry provides relative density contrasts within each scan but not absolute bone density values. Color scales reflect relative attenuation, primarily distinguishing dense cortical bone from trabecular bone and infilling matrix, but are not standardized across different specimens due to potential

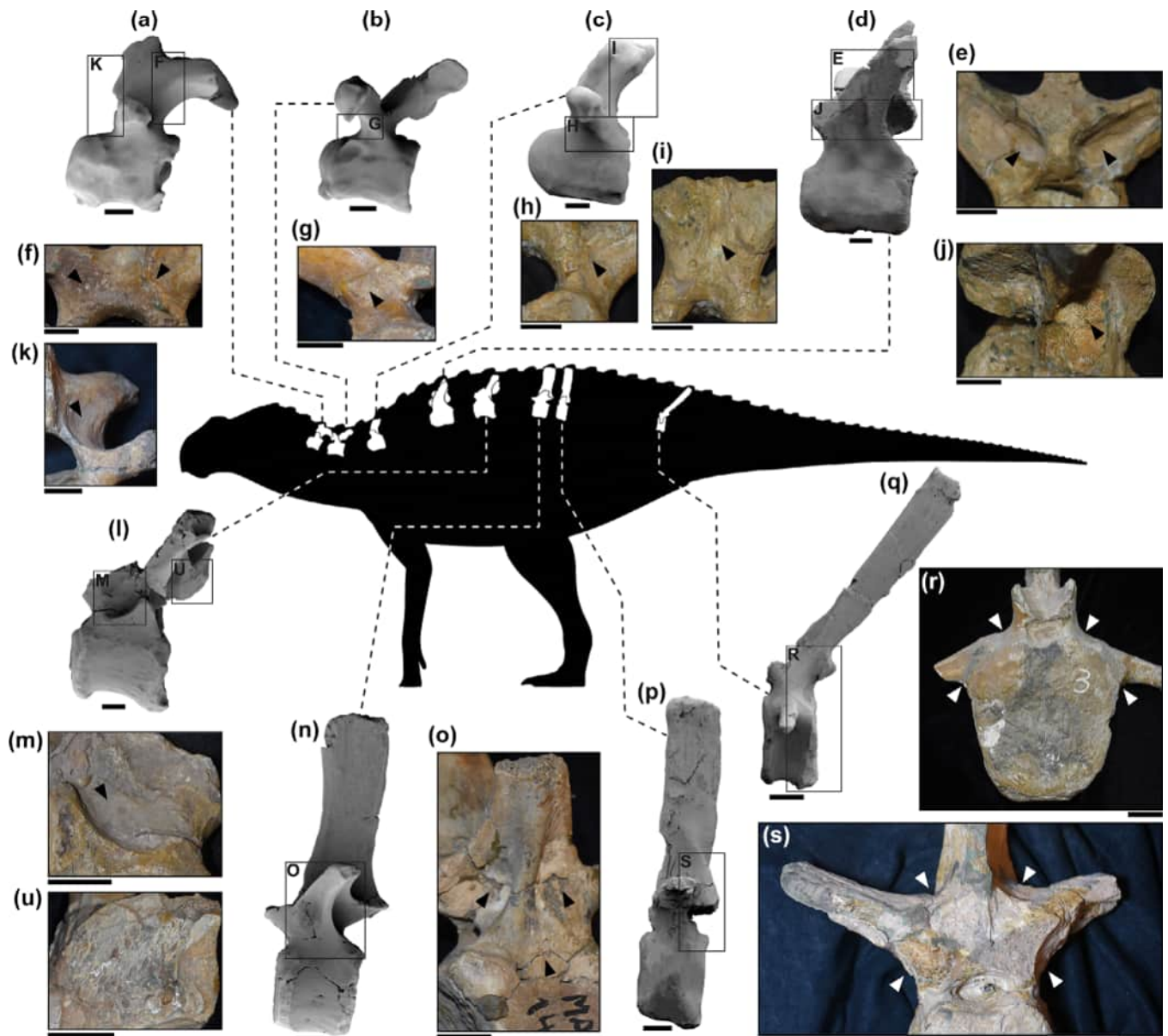


FIGURE 1 Reconstruction of the saurolophine hadrosaur *Huallasaurus australis* showing the cervical (a–c,f,i,k), dorsal (d,e,j,l–p,s,u), and caudal (q,r) vertebrae analyzed in this study. Three-dimensional reconstructions from CT scans in (a–d,l,n,p,q). MACN-Pv RN02.a in (a,f,k); MACN-Pv RN02.b in (b,g); MACN-Pv RN826.a in (c,h,i); MACN-Pv RN826.b in (d,e,j); MACN-Pv RN02.c in (l,m,u); MACN-Pv RN146.a in (l,m,u); MACN-Pv RN826.c in (p,s); MACN-Pv RN02.d in (q,r). Photographs showing blind fossae in (e–k,m,o,r,s) (arrows). Detail of a worn portion of the neural arch exposing an internal pneumatic trabecular architecture (u). Left lateral view in (a–d,l,n,p,q). Right lateral view in (j,m,o). Caudal view in (e–i,r,s). Cranial view in K. Scale bar = 20 mm. Reconstruction is not to scale.

variation in fossilization and matrix composition. Therefore, we opted for a qualitative approach since mineral infills in bone pores and diagenetic differences between specimens hinder quantitative analyses. We used 3D Slicer version 5.2.1 for the scan analyses (Fedorov et al., 2012) and CloudCompare (Girardeau-Montaut, 2016) for generating the 3D model reconstructions seen in Figure 1. Given the voxel resolution of 0.75 mm, fine-scale trabecular details are visible in larger vertebral regions but may be underestimated in thinner cortical structures or small features. All interpretations are therefore conservative with respect to resolution limitations. All scans were uploaded to Morphobank and are available for download through this link: <https://www.morphosource.org/projects/000698046>.

3 | RESULTS

The CT scans of *Huallasaurus* revealed the microanatomy preserved without major diagenetic artifacts (Figures 2–4), except for MCN-PV RN 02.b and MCN-PV RN 186.a and 02.b, in which minerals caused visual anomalies in some portions (Figures 2a,c,h and 3a–d,f). Notwithstanding, the internal architecture of all vertebrae could be visualized (Figures 2–4).

The cervical vertebrae present a few laminae with shallow blind fossae in the neural arch (Figure 1a–c,f–i,k). The centra show no lateral fossae. There are two small parallel craniocaudally elongated vascular foramina in the right lateral centrum of MACN-Pv RN 02.b. The internal structure shows dense trabecular bone matrix without pneumatic cavities throughout the vertebra (Figure 2).

The anterior to middle dorsal vertebrae present laminae with slightly deeper centrodiapophyseal fossae compared with the cervicals (Figure 1d,l). Spinodiapophyseal fossae are very shallow. However, all fossae are blind (Figure 1e,j,m). The centra present no lateral fossae. A fortuitous break exposes a dense trabecular array inside the neural arch of MACN-Pv RN02 (Figure 1u). The internal structure comprises a trabecular bone matrix of moderate density, without evidence of pneumatic chambers (Figure 3). However, there is a noticeable decrease in trabecular density in the areas under the spinodiapophyseal fossae and the neural spine, compared to the cervical vertebrae (Figure 3a–d).

The posterior-most dorsal vertebra MACN-Pv RN146.a presents laminae with slightly deep centrodiapophyseal fossae as observed in the anterior to middle dorsals (Figure 1n,o). The posterior-most dorsal vertebra MACN-Pv RN826.c and the anterior caudal MACN-Pv RN02.d present shallow to nearly absent centrodiapophyseal and spinodiapophyseal fossae (Figure 1p–s). Nevertheless, all fossae are still blind (Figures 1n–s and 4). The centra of MACN-Pv RN146.a and MACN-Pv RN02.d present no lateral fossae.

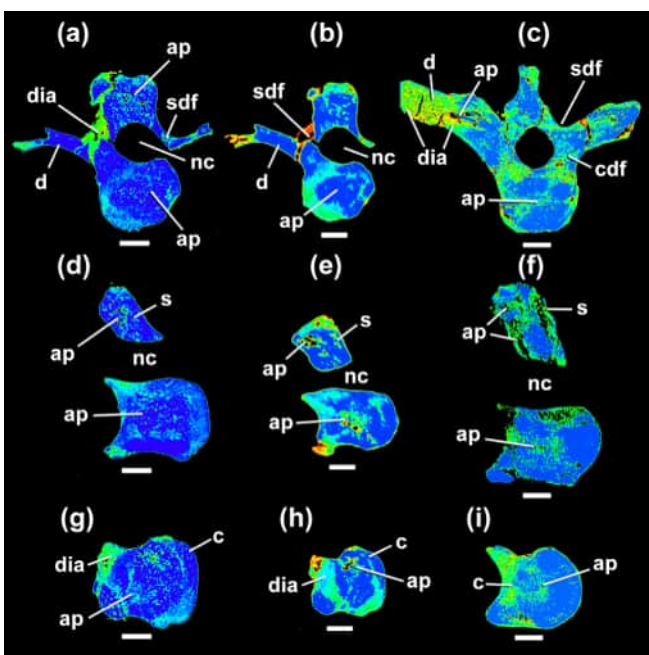


FIGURE 2 Computed tomography densitometry analysis of the hadrosaur *Huallasaurus* cervical vertebrae in transverse (a–c), parasagittal (d–f) and frontal (g–i) views. MACN-Pv RN02.a in (a,d, g). MACN-Pv RN02.b in (b,e,h). MACN-Pv RN826.a in (c,f,i). Note the absence of deep fossae connecting to large internal chambers, demonstrating the lack of PSP in the elements. Lighter blue and green indicate lower densities (e.g., small apneumatic chambers). Darker blue illustrates denser structures (e.g., compact bone tissue, dense trabecular matrix etc). Note that variations may occur due to diagenetic artifacts. ap, apneumatic bone; c, centrum; cdf, centrodiapophyseal fossa; d, diapophysis; dia, diagenetic artifacts; nc, neural canal; s, neural spine; sdf, spinodiapophyseal fossa. Scale bar = 20 mm.

There are three small parallel craniocaudally elongated lateral vascular foramina in the centrum of MACN-Pv RN826. c. Internally, the vertebrae exhibit an apneumatic trabecular matrix that remains relatively dense across the centra and neural arches, with no evidence of internal pneumatic cavities (Figure 4). The tall neural spines present a thick cortical architecture in most of their extension (Figure 4a–f). Cortical walls are reduced in the centra and in the extremities of the diaphyses and the neural spines in both the posterior-most dorsals and the anterior caudal.

4 | DISCUSSION

4.1 | Evolution of the dinosauriform vertebral microanatomy

Our results show no evidence of internal pneumatic structures in *Huallasaurus* vertebrae. The overall density

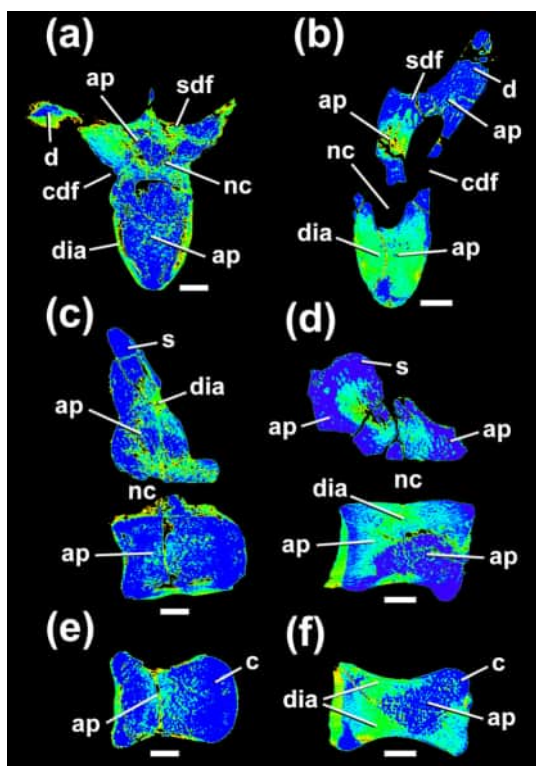


FIGURE 3 Computed tomography densitometry analysis of the hadrosaur *Huallasaurus* anterior to middle dorsal vertebrae in transverse (a,b), parasagittal (c,d) and frontal (e,f) views. MACN-Pv RN826.b in (a,c,e). MACN-Pv RN02.c in (b,d,f). Note the absence of deep fossae connecting to large internal chambers, demonstrating the lack of PSP in the vertebrae. Lighter blue and green indicate lower densities (e.g., small apneumatic trabeculae). Darker blue illustrates denser structures (e.g., compact bone tissue, dense trabecular matrix etc). Note that variations may occur due to diagenetic artifacts. ap, apneumatic bone; c, centrum; cdf, centrodiapophyseal fossa; d, diaphysis; dia, diagenetic artifacts; nc, neural canal; s, neural spine; sdf, spinodiapophyseal fossa. Scale bar = 20 mm.

of the trabecular array is less compact than in the centra of the archosauriforms *Stenaulorhynchus* NHMUK R36618, *Erythrosuchus* NHMUK R3592, and the Phylosauria indet. NHMUK OR38072 (Butler et al., 2012). However, the vertebrae of *Huallasaurus* were denser than in the herrerasaurid *Gnathovorax* CAPPA/UFSM 0035 and in the early sauropodomorphs *Buriolestes* CAPPA/UFSM 0035 and *Pampadromaeus* ULBRA-PV016 (Aureliano et al., 2022). Also, the vertebrae were less vascularized than the condition seen in the early thyreophoran *Scelidosaurus* NHMUK R1111, especially the caudals (Butler et al., 2012). Interestingly, the internal apneumatic architecture of *Huallasaurus* appears superficially similar to that observed in the silesaurid ZPAL Ab III vertebral series (Butler et al., 2012), sharing even the tiny centripetal circumferential chambers and the vascularized clusters surrounding the cotyles (Figure 5).

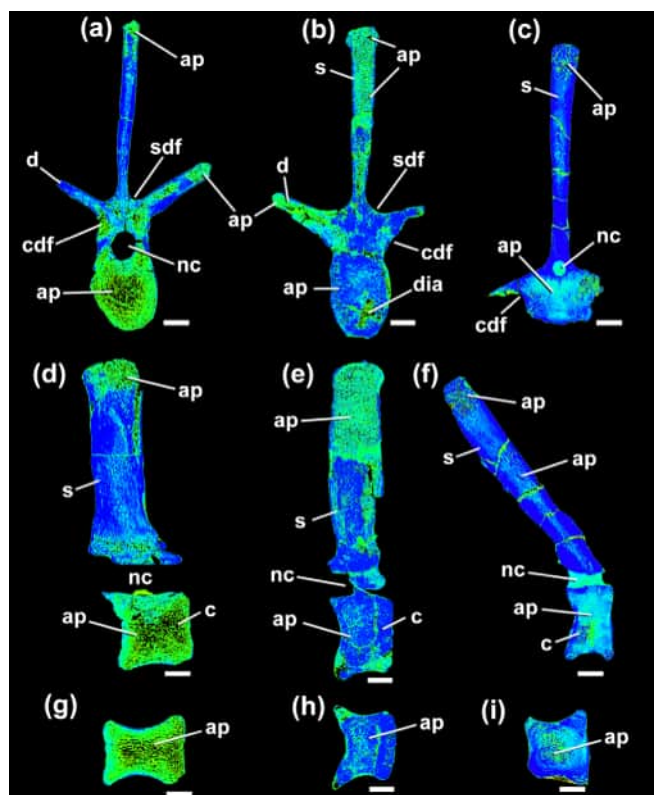


FIGURE 4 Computed tomography densitometry analysis of the hadrosaur *Huallasaurus* posterior dorsal (a,b,d,e,g,h) and caudal (c,f,i) vertebrae in transverse (a–c), parasagittal (d–f), and frontal (g–i) views. MACN-Pv RN146.a in (a,d,g). MACN-Pv RN826.c in (b,e,h). MACN-Pv RN02.d in (c,f,i). Note the absence of deep fossae connecting to large internal chambers, demonstrating the lack of PSP in the vertebrae. Lighter blue and green indicate lower densities (e.g., small apneumatic trabeculae). Darker blue illustrates denser structures (e.g., compact bone tissue, dense trabecular matrix etc). Variations may occur due to diagenetic artifacts. ap, apneumatic bone; c, centrum; cdf, centrodiapophyseal fossa; d, diaphysis; dia, diagenetic artifacts; nc, neural canal; s, neural spine; sdf, spinodiapophyseal fossa. Scale bar = 20 mm.

Variation in trabecular architecture across cervical, dorsal, and caudal vertebrae may reflect biomechanical loading or positional anatomy differences rather than evolutionary signals alone. Furthermore, given the different sizes of the specimens, potential ontogenetic effects cannot be ruled out.

4.2 | Evolution of the ornithischian respiration

Anatomical evidence from *Heterodontosaurus tucki* (AM 4766 and SAM-PK-K1332) suggested the “pelvic bellows” model for ornithischian ventilation (Radermacher et al., 2021). *Heterodontosaurus tucki* exhibits reduced

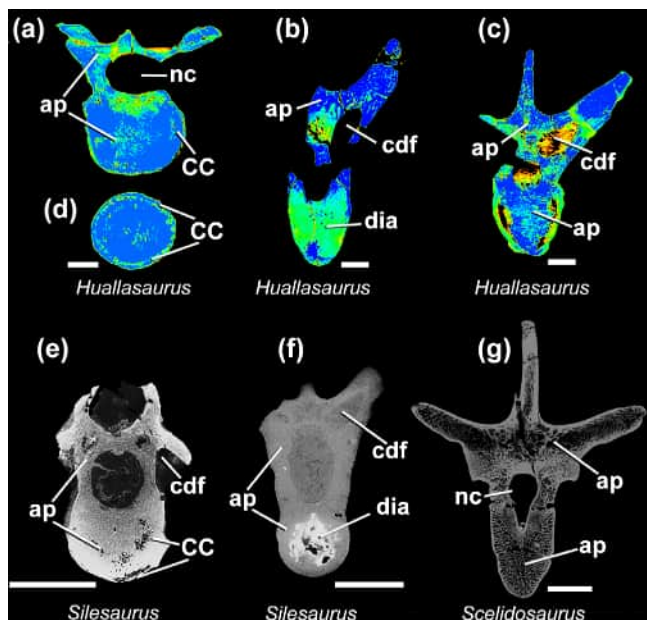


FIGURE 5 CT scan slices comparison between the vertebrae of ornithischians and *Silesaurus*. The hadrosaur *Huallasaurus* MACN-Pv RN826.a (a,d); MACN-Pv RN826.b (b); MACN-Pv RN 02.c (c). *Silesaurus* ZPAL Ab III 1299 (e); ZPAL Ab III 423/6 (f) (Butler et al., 2012). (g) The thyreophoran *Scelidosaurus* NHMUK R1111 (Butler et al., 2012). Cervical vertebrae in (a–c). Dorsal vertebrae in (b,c, f,g). All in transverse view. ap, apneumatic bone; cc, circumferential chambers; cdf, centrodiaphyseal fossa; dia, diagenetic artifacts; nc, neural canal. Scale bar in a–d,g = 20 mm; in e,f = 10 mm.

gastralia, an elaborate sternum, mobile sternal ribs, and an incipient anterior pubic process (APP), indicating a transition from cuirassal breathing (Radermacher et al., 2021). Early ornithischians likely used a “puboperitoneal muscle” attached to the APP as an accessory ventilator. Later genasaurs (i.e., hadrosaurs) lost gastralia, and APP elongation suggested this muscle became the primary ventilator. Vertebrocostal orientations indicated a bipartite, dorsally immobile lung, unlike the crocodilian hepatic piston, but convergent in pelvic involvement, with the puboperitoneal muscle acting on flexible lung regions.

The vertebral morphology of ornithischian dinosaurs provides additional support for this respiratory model. Analysis of costovertebral joint anatomy across archosaurs reveals that ornithischians, like other non-avian dinosaurs, possessed separate parapophyses and diapophyses throughout their dorsal vertebral series, creating a furrowed thoracic ceiling similar to that of modern birds (Brocklehurst et al., 2020; Schachner et al., 2011). This contrasts with the smooth thoracic ceiling of crocodilians, where parapophyses migrate onto transverse processes, allowing greater lung mobility during hepatic piston ventilation (Brocklehurst et al., 2020). The furrowed thoracic ceiling in ornithischians would have provided structural support for dorsally immobile, heterogeneously partitioned lungs with a rigid

dorsocranial region containing the majority of gas-exchange tissue, ventilated by a more flexible and less vascularized caudal region (Schachner et al., 2011).

The evolution of ornithischian respiratory mechanics likely involved a transition from the ancestral cuirassal breathing mechanism proposed for basal archosaurs, which utilized the gastralia basket and ischiotruncus muscle for ventilation (Schachner et al., 2011), to the specialized pelvic bellows system. This transition is evidenced by the progressive reduction and eventual loss of gastralia in more derived ornithischians, coupled with the development of the APP and associated musculature (Radermacher et al., 2021).

Our observations in *Huallasaurus* are consistent with the hypothesis that invasive air sac diverticula did not evolve in Ornithischia, in which the apneumatic postcranial skeleton remained a plesiomorphic adaptation inherited from their Triassic ancestors. Our finding is compatible with the “pelvic bellows” model for ornithischian ventilation (Radermacher et al., 2021) and with previous evidence suggesting multiple origins (Figure 6) for the evolution of the PSP in ornithodirans (Aureliano et al., 2022, 2023; Butler et al., 2012).

4.3 | Remarks on dinosaur systematics

Some studies suggested a paraphyletic condition for silesaurs, recovering them as early-diverging ornithischians (Cabreira et al., 2016; Cau, 2024; Müller & Garcia, 2020; Norman et al., 2022). This hypothesis also finds support in morphological data, since the PSP is present in post-Carnian saurischians but seemingly absent in ornithischians, based on both macroscopic observations and tomography of Jurassic taxa *Heterodontosaurus* (Radermacher et al., 2021) and *Scelidosaurus* (Butler et al., 2012). Our results now suggest that *Huallasaurus*, and possibly other hadrosauriforms, did not only retain an internal vertebral microanatomy similar to Triassic archosauriforms, but shared the vascular pattern with *Silesaurus* more than with any other archosauriforms (Figure 6). Therefore, our results may contribute to the ongoing discussion regarding the paraphyletic condition of early dinosaurs, particularly with respect to internal vertebral microanatomy, although this should be tested further with broader sampling.

4.4 | Remarks on hadrosaur vertebral morphology

The analyses of *Huallasaurus* vertebrae reveal a trabecular bone arrangement that appears denser than that observed in several other dinosaur taxa examined in previous studies, although this may reflect biomechanical

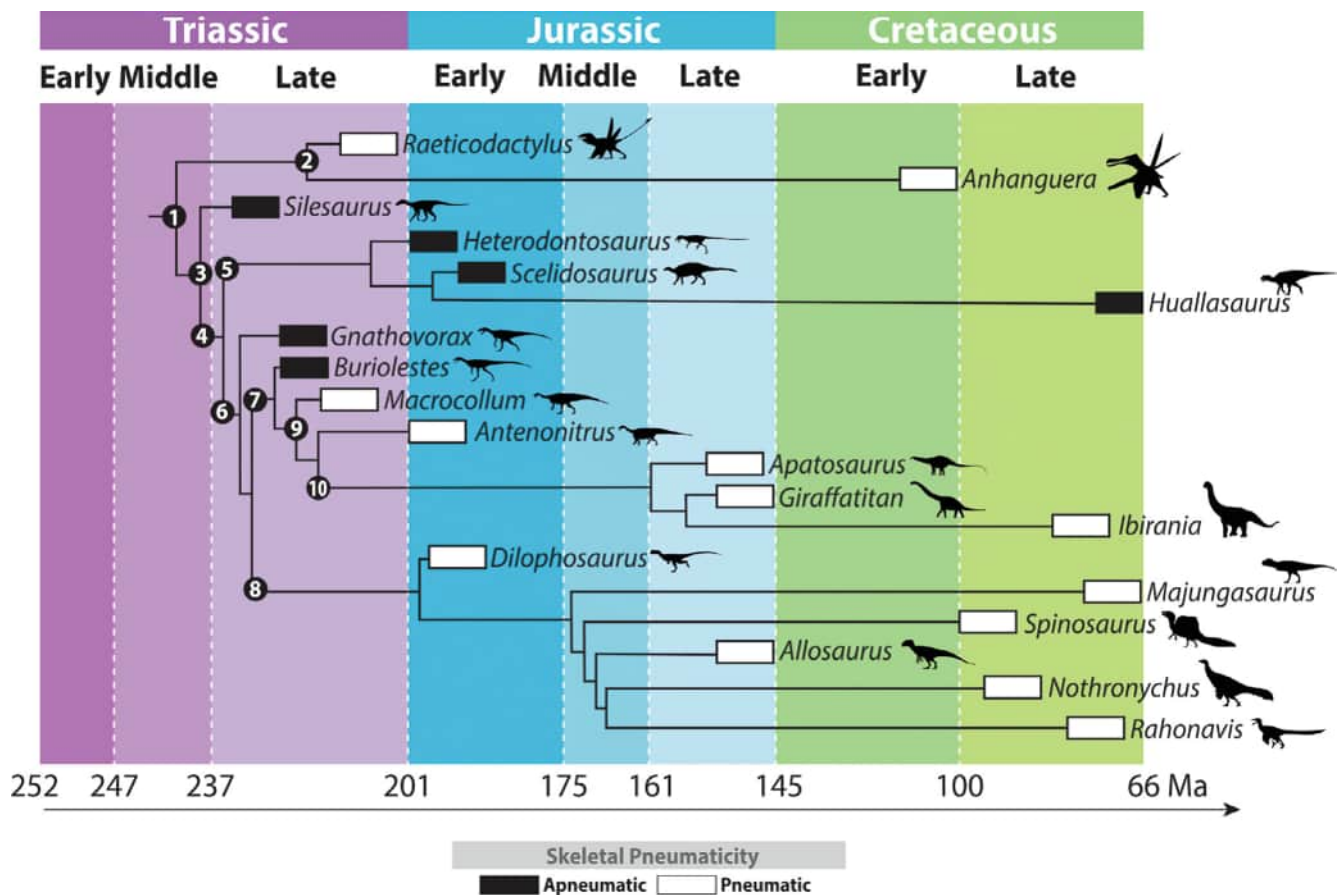


FIGURE 6 Chronological and phylogenetic evolution of postcranial skeletal pneumaticity in ornithodirans. 1, Ornithodira; 2, Pterosauria; 3, Dinosauromorpha; 4, Dinosauria; 5, Ornithischia; 6, Saurischia; 7, Sauropodomorpha; 8, Theropoda; 9, Plateosauria; 10, Sauropoda. *Allosaurus* (Smith et al., 2021), *Apatosaurus* (Wedel & Taylor, 2013), *Anhanguera* (Buchmann et al., 2021), *Antenonitrus* (Yates et al., 2012), *Buriolestes* (Aureliano et al., 2022), *Dilophosaurus* (Marsh & Rowe, 2020), *Giraffatitan* (Wedel & Taylor, 2013), *Gnathovorax* (Aureliano et al., 2022), *Heterodontosaurus* (Radermacher et al., 2021), *Ibirania* (Aureliano et al., 2021), *Macrocollum* (Aureliano et al., 2023), *Majungasaurus* (Aureliano et al., 2024; O'Connor, 2006), *Nothronychus* (Smith et al., 2021), *Raeticodactylus* (Butler et al., 2009), *Rahonavis* (Aureliano et al., 2024; Forster et al., 2020), *Scelidosaurus* (Butler et al., 2012), *Silesaurus* (Butler et al., 2012), and *Spinosaurus* (Myhrvold et al., 2024). (Aureliano et al., 2024; Forster et al., 2020). Silhouettes are from Phylopic.org by Alessio Ciolfi, Cy Marchant, Iain Reid, Jaime Headden, JF Designs, Julio Garza, Mathew Wedel, Matthew Dempsey, Tasman Dixon, Walter Vladimir, and Will Toosey. Adapted from Aureliano et al. (2023).

adaptations, taxon-specific factors, or ontogenetic stages. The presence of a dense trabecular matrix and the absence of large internal chambers throughout the vertebral series represent a condition that, intriguingly, shows superficial similarity to that observed in large mammals, including the domestic bull (*Bos taurus*), the North American deer (*Odocoileus virginianus*), and the orca whale (*Orcinus orca*) (Figure 7). Likewise, the extreme reduction of cortical walls in the centra and certain regions of the neural spines mirrors a condition seen in aquatic mammals such as cetaceans (Buffrénil & Schoevaert, 1988).

This reduction in total cortical bone volume, paired with the expansion of a lightweight yet dense trabecular matrix, reflects an architecture that decreases body density while maintaining structural integrity (Fabbri et al., 2022;

Houssaye et al., 2015, 2016; Myhrvold et al., 2024). In extant mammals, such trabecular spaces are frequently occupied by marrow tissues, including fat and hematopoietic cells, functioning as intraosseous energy reserves (Butler et al., 2012; O'Connor, 2006; Prothero, 1995). The absence of PSP in *Huallasaurus*, and most likely in other hadrosaurs, added to this dense internal trabecular matrix, aiding these organisms in the evolution of large body sizes and extra stocks of fat. While we cannot directly confirm the presence of such fatty deposits in *Huallasaurus*, it is plausible that the dense trabecular network could have supported similar metabolic functions, particularly given isotopic evidence suggesting regional migratory behaviors in hadrosaurs (Terrill et al., 2020), as observed in modern migratory mammals (Prothero, 1995).

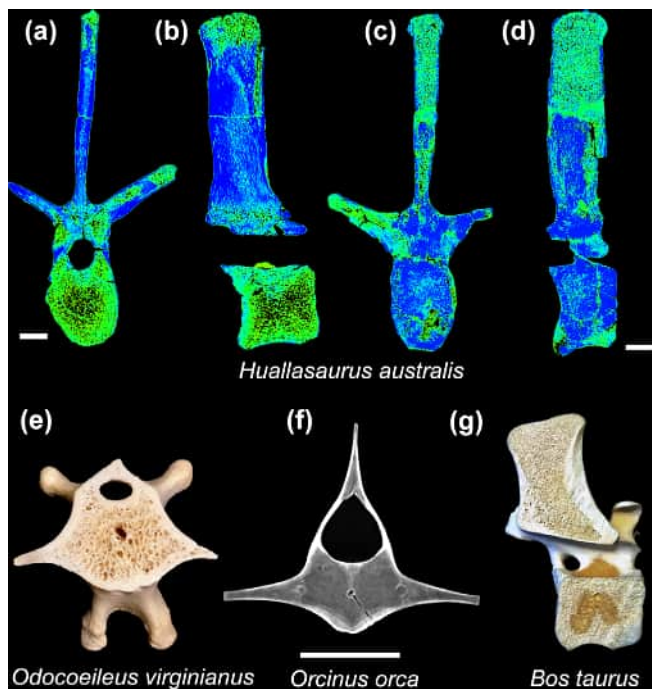


FIGURE 7 Comparison between the dense trabecular tissue in the vertebrae of the hadrosaur *Huallasaurus australis* (a–d) and the internal structures in modern mammals (e–g). (e) Bone cross section of *Odocoileus virginianus*, a North American deer (unnumbered; courtesy of Mathew Wedel). (f) CT scan of *Orcinus orca*, the orca whale (lumbar; CEM 038977; courtesy of Gabriel L. Gomes). (g) Bone cross section of *Bos taurus*, the domestic bull (unnumbered; courtesy of Mathew Wedel). Transverse view in (a, c, e, f). Parasagittal view in (b,d,g). Scale bar in (a–d) = 20 mm; in (f) = 10 mm. (e,g) Not to scale.

Importantly, this hypothesis remains speculative and requires further testing through broader sampling of hadrosaur vertebral microanatomy, ideally incorporating histological sections to directly assess bone marrow space and tissue composition. Nevertheless, our observations provide a compelling foundation for considering how skeletal architecture may have interacted with ecological and physiological demands in large-bodied ornithischians.

4.5 | Vertebral internal structure and body size evolution in dinosaurs

The remarkable evolutionary success of hadrosaurs in achieving large body sizes without PSP provides compelling evidence that extensive pneumatization represents an advantageous rather than essential adaptation for dinosaur gigantism. *Shantungosaurus giganteus*, reaching 16 m in length and weighing 15 metric tons, represents one of the largest terrestrial herbivores ever recorded,

demonstrating that alternative skeletal architectures could support extreme body sizes without the respiratory adaptations that characterized saurischian giants (Hu, 1973; Xu et al., 2000). The dense trabecular matrix observed in hadrosaur vertebrae likely represents a biomechanical solution to the structural challenges of large body size in the absence of pneumatic weight reduction, paralleling the trabecular architecture seen in large mammals where trabecular density increases rather than trabecular thickness as body size scales up (Aguirre et al., 2020; Barak et al., 2013). While sauropods achieved gigantism through extensive PSP that reduced body density while maintaining structural integrity, hadrosaurs evolved a different strategy, utilizing dense, apneumatic trabecular architecture (Aureliano et al., 2021; Butler et al., 2012; Cerda et al., 2012; Wedel, 2003). The comparative body size data support this hypothesis, as moderately large dinosaurs like *Tyrannosaurus rex* achieved comparable dimensions to the largest hadrosaurs despite possessing extensive pneumatization, whereas the truly gigantic sauropods like *Argentinosaurus*, reaching lengths of over 30 m and masses exceeding 30 tons, likely required the extreme body density reduction provided by extensive pneumatization to achieve such unprecedented sizes (Campione & Evans, 2012; D'Emic, 2023). This suggests a threshold effect where PSP becomes increasingly critical as body size approaches the upper limits of terrestrial vertebrate physiology, with multiple evolutionary pathways leading to dinosaur gigantism representing different solutions to the biomechanical challenges of large body size.

4.6 | Limitations and future directions

We acknowledge that our discussions are based on a limited number of vertebrae from three individuals of varying sizes and uncertain ontogenetic stages. Additionally, differences in vertebral region (cervical, dorsal, caudal) and potential taphonomic alterations may influence trabecular architecture. The medical-grade CT (0.75 mm voxels) allowed broad qualitative assessments but lacked the resolution necessary to quantify cortical thickness, trabecular spacing, and the precise volume of any trabecular cavities. Future work using high-resolution micro-CT ($\leq 50 \mu\text{m}$ voxels) will enable voxel-based morphometry of these parameters, particularly in delicate neural spine apices and centrum cortices. Likewise, histological thin sections cut through the centrum and neural arch could directly reveal marrow composition, secondary osteon density, and possible growth lines, providing a tissue-level test of the fat-storage hypothesis.

5 | CONCLUSION

The microanatomical analysis of the vertebrae of *H. australis* provides valuable insights into the evolution of skeletal structure in ornithischian dinosaurs. The internal architecture of the axial skeleton exhibits an apneumatic trabecular matrix distributed throughout the centrum and neural arch, without signs of internal pneumatic chambers, contrasting sharply with the pneumatized condition characteristic of post-Carnian saurischians.

Our observations reveal that the vertebral vascular pattern in *Huallasaurus* bears a notable resemblance to that of *Silesaurus*. Whether this similarity reflects deep phylogenetic relationships or convergent functional adaptations remains an open question that warrants further investigation.

Additionally, the expanded trabecular matrix coupled with remarkably thin cortical walls observed in *Huallasaurus* shows superficial similarity to the vertebral architecture of large modern mammals, which often accommodate intraosseous fat deposits. While the functional implications of this condition in *Huallasaurus* remain speculative, it may represent a biomechanical or physiological adaptation associated with supporting large body size in an apneumatic skeleton.

Given the limited sample size, the inclusion of vertebrae from different anatomical regions, and uncertain ontogenetic stages of the specimens, these conclusions should be regarded as preliminary. Nonetheless, this study highlights the potential for vertebral microanatomy to inform broader questions about respiratory evolution, body mass adaptations, and phylogenetic relationships in ornithischians. Future research incorporating histological sections, higher-resolution imaging, and a wider taxonomic sampling across Ornithischia and Silesauridae will be crucial for testing the patterns and hypotheses proposed herein.

AUTHOR CONTRIBUTIONS

Tito Aureliano: Conceptualization; investigation; funding acquisition; writing – original draft; methodology; validation; visualization; writing – review and editing; software; formal analysis; project administration. **Aline M. Ghilardi:** Conceptualization; funding acquisition; investigation; methodology; validation; writing – review and editing; supervision; formal analysis. **Jonatan Kaluza:** Investigation; visualization; formal analysis; software; funding acquisition; validation. **Agustín G. Martinelli:** Data curation; supervision; resources; funding acquisition; investigation; methodology; formal analysis; writing – original draft; writing – review and editing; validation.

ACKNOWLEDGMENTS

The authors are grateful to the following funding agencies: Fundação Norte-Rio-Grandense de Pesquisa e Cultura (FUNPEC-UFRN/PIB21712-2023) (A.M.G.), Fundação Cearense de Apoio ao Desenvolvimento Científico e Tecnológico (FUNCAP/FPD-0213-00295.01.01/23) (T.A.), and CONICET (J.K., A.G.M.). We thank Guilhermo Windholz for the comments on an earlier version of this study. We thank Adrián Giacchino, Cristian Rizzo, Cristian Granson, Mora Loto, Paula Muzzopappa, and the Fundación de Historia Natural “Félix de Azara” for their assistance in conducting the computed tomography scans at the Universidad Maimónides (Buenos Aires, Argentina) of the specimens studied here. The Article Processing Charge for the publication of this research was funded by the Coordenação de Aperfeiçoamento de Pessoal de Nível Superior - Brasil (CAPES) (ROR identifier: 00x0ma614).

CONFLICT OF INTEREST STATEMENT

The authors declare no competing interests.

DATA AVAILABILITY STATEMENT

The specimen is housed in a public research institution and can be accessed upon request to the collection's curator. Tomography data are available in Morphosource (links provided in Materials and Method).

ORCID

Tito Aureliano  <https://orcid.org/0000-0002-6918-0519>

Aline M. Ghilardi  <https://orcid.org/0000-0001-9136-0236>

Jonatan Kaluza  <https://orcid.org/0000-0002-5945-0044>

Agustín G. Martinelli  <https://orcid.org/0000-0003-4489-0888>

REFERENCES

- Aguirre, T. G., Ingrole, A., Fuller, L., Seek, T. W., Fiorillo, A. R., Sertich, J. J. W., & Donahue, S. W. (2020). Differing trabecular bone architecture in dinosaurs and mammals contribute to stiffness and limits on bone strain. *PLoS One*, 15, e0237042.
- Aureliano, T., Almeida, W., Rasaona, M., & Ghilardi, A. M. (2024). The evolution of the air sac system in theropod dinosaurs: Evidence from the Upper Cretaceous of Madagascar. *Journal of Anatomy*. <https://doi.org/10.1111/joa.14113>
- Aureliano, T., Ghilardi, A. M., Müller, R. T., Kerber, L., Fernandes, M. A., Ricardi-Branco, F., & Wedel, M. J. (2023). The origin of an invasive air sac system in sauropodomorph dinosaurs. *Anatomical Record*, 307, 1084–1092. <https://doi.org/10.1002/ar.25209>
- Aureliano, T., Ghilardi, A. M., Müller, R. T., Kerber, L., Pretto, F. A., Fernandes, M. A., Ricardi-Branco, F., & Wedel, M. J. (2022). The absence of an invasive air sac system in the earliest dinosaurs suggests multiple origins of vertebral pneumaticity. *Scientific Reports*, 12, 20844.

- Aureliano, T., Ghilardi, A. M., Navarro, B. A., Fernandes, M. A., Ricardi-Branco, F., & Wedel, M. J. (2021). Exquisite air sac histological traces in a hyperpneumatized nanoid sauropod dinosaur from South America. *Scientific Reports*, 11, 24207.
- Aureliano, T., Ghilardi, A. M., Silva-Junior, J. C. G., Martinelli, A. G., Ribeiro, L. C. B., Marinho, T., Fernandes, M. A., Ricardi-Branco, F., & Sander, P. M. (2020). Influence of taphonomy on histological evidence for vertebral pneumaticity in an Upper Cretaceous titanosaur from South America. *Cretaceous Research*, 108, 104337.
- Barak, M. M., Lieberman, D. E., & Hublin, J.-J. (2013). A Wolff in sheep's clothing: Trabecular bone adaptation in response to changes in joint loading orientation. *Bone*, 53, 1–10.
- Bonaparte, J. F., Franchi, M. R., Powell, J. E., & Sepulveda, E. G. (1984). La Formación Los Alamitos (Campaniano-Maastrichtiano) del sudeste de Río Negro, con descripción de *Kritosaurus australis* n. sp. (Hadrosauridae). Significado paleogeográfico de los vertebrados. *Revista de la Asociación Geológica Argentina*, 39, 284–299.
- Bonaparte, J. F., & Rougier, G. (1987). Late Cretaceous fauna Los Alamitos, Patagonia, Argentina. VII: hadrosaurs. *Revista del Museo Argentino de Ciencias Naturales Bernardino Rivadavia e Instituto Nacional de Investigación de Las Ciencias Naturales*, 3, 155–161.
- Britt, B. B. (1993). Pneumatic postcranial bones in dinosaurs and other archosaurs. [Ph.D. thesis]. University of Calgary.
- Brochu, C. A. (1996). Closure of neurocentral sutures during crocodylian ontogeny: Implications for maturity assessment in fossil archosaurs. *Journal of Vertebrate Paleontology*, 16, 49–62.
- Brocklehurst, R. J., Schachner, E. R., Codd, J. R., & Sellers, W. I. (2020). Respiratory evolution in archosaurs. *Philosophical Transactions of the Royal Society of London. Series B, Biological Sciences*, 375, 20190140.
- Buchmann, R., Holgado, B., Sobral, G., Dos Santos Avilla, L., & Rodrigues, T. (2021). Quantitative assessment of the vertebral pneumaticity in an anhanguerid pterosaur using micro-CT scanning. *Scientific Reports*, 11, 18718.
- Buffrénil, V., & Schoevaert, D. (1988). On how the periosteal bone of the delphinid humerus becomes cancellous: Ontogeny of a histological specialization. *Journal of Morphology*, 198, 149–164.
- Butler, R. J., Barrett, P. M., & Gower, D. J. (2009). Postcranial skeletal pneumaticity and air-sacs in the earliest pterosaurs. *Biology Letters*, 5, 557–560.
- Butler, R. J., Barrett, P. M., & Gower, D. J. (2012). Reassessment of the evidence for postcranial skeletal pneumaticity in Triassic archosaurs, and the early evolution of the avian respiratory system. *PLoS One*, 7, e34094.
- Cabreira, S. F., Kellner, A. W. A., Dias-da-Silva, S., Roberto da Silva, L., Bronzati, M., Marsola, J. C. d. A., Müller, R. T., de Souza Bittencourt, J., Jul'Armando Batista, B., Raugust, T., Carrilho, R., Brodt, A., & Langer, M. C. (2016). A unique Late Triassic dinosauromorph assemblage reveals dinosaur ancestral anatomy and diet. *Current Biology: CB*, 26, 3090–3095.
- Campione, N. E., & Evans, D. C. (2012). A universal scaling relationship between body mass and proximal limb bone dimensions in quadrupedal terrestrial tetrapods. *BMC Biology*, 10, 60.
- Cau, A. (2024). A unified framework for predatory dinosaur macroevolution. *Bollettino Della Società Paleontologica Italiana*, 63(2), 1–19.
- Cerdá, I. A., Salgado, L., & Powell, J. E. (2012). Extreme postcranial pneumaticity in sauropod dinosaurs from South America. *Paläontologische Zeitschrift*, 86, 441–449.
- D'Emic, M. D. (2023). The evolution of maximum terrestrial body mass in sauropod dinosaurs. *Current Biology*, 33, 1824–1830.
- Fabbri, M., Navalón, G., Benson, R. B. J., Pol, D., O'Connor, J., Bhullar, B.-A. S., Erickson, G. M., Norell, M. A., Orkney, A., Lamanna, M. C., Zouhri, S., Becker, J., Emke, A., Sasso, C. D., Bindellini, G., Maganuco, S., Auditore, M., & Ibrahim, N. (2022). Subaqueous foraging among carnivorous dinosaurs. *Nature*, 603, 852–857.
- Fedorov, A., Beichel, R., Kalpathy-Cramer, J., Finet, J., Fillion-Robin, J.-C., Pujol, S., Bauer, C., Jennings, D., Fennessy, F., Sonka, M., Buatti, J., Aylward, S., Miller, J. V., Pieper, S., & Kikinis, R. (2012). 3D slicer as an image computing platform for the quantitative imaging network. *Magnetic Resonance Imaging*, 30, 1323–1341.
- Forster, C., O'Connor, P., Chiappe, L., & Turner, A. (2020). The osteology of the Late Cretaceous paravian *Rahonavis ostromi* from Madagascar. *Palaeontologia Electronica*, 23(2), a29. <https://doi.org/10.26879/793>
- Girardeau-Montaut, D. (2016). CloudCompare. France: EDF R&D Telecom ParisTech, 11. https://pcp2019.ifp.uni-stuttgart.de/presentations/04-CloudCompare_PCP_2019_public.pdf
- Hone, D. W. E., Farke, A. A., & Wedel, M. J. (2016). Ontogeny and the fossil record: What, if anything, is an adult dinosaur? *Biology Letters*, 12, 20150947.
- Houssaye, A., Sander, P. M., & Klein, N. (2016). Adaptive patterns in aquatic amniote bone microanatomy—More complex than previously thought. *Integrative and Comparative Biology*, 56, 1349–1369.
- Houssaye, A., Tafforeau, P., de Muizon, C., & Gingerich, P. D. (2015). Transition of Eocene whales from land to sea: Evidence from bone microstructure. *PLoS One*, 10, e0118409.
- Hu, C.-C. (1973). A new hadrosaur from the Cretaceous of Chucheng, Shantung. *Acta Geologica Sinica*, 1973, 179–206.
- Maina, J. N. (2006). Development, structure, and function of a novel respiratory organ, the lung-air sac system of birds: To go where no other vertebrate has gone. *Biological Reviews of the Cambridge Philosophical Society*, 81, 545–579.
- Marsh, A. D., & Rowe, T. B. (2020). A comprehensive anatomical and phylogenetic evaluation of *Dilophosaurus wetherilli* (Dinosauria, Theropoda) with descriptions of new specimens from the. *Journal of Paleontology*, 94, 1–103.
- Müller, R. T., & Garcia, M. S. (2020). A paraphyletic "Silesauridae" as an alternative hypothesis for the initial radiation of ornithischian dinosaurs. *Biology Letters*, 16, 20200417.
- Myhrvold, N. P., Baumgart, S. L., Vidal, D., Fish, F. E., Henderson, D. M., Saitta, E. T., & Sereno, P. C. (2024). Diving dinosaurs? Caveats on the use of bone compactness and pFDA for inferring lifestyle. *PLoS One*, 19, e0298957.
- Norman, D. B., Baron, M. G., & Garcia, M. S. (2022). Taxonomic, palaeobiological and evolutionary implications of a phylogenetic hypothesis for Ornithischia (Archosauria: Dinosauria). *Zoological Journal of the Linnean Society*, 194, 1273–1309.
- O'Connor, P. M. (2006). Postcranial pneumaticity: An evaluation of soft-tissue influences on the postcranial skeleton and the reconstruction of pulmonary anatomy in archosaurs. *Journal of Morphology*, 267, 1199–1226.

- Perry, S. F., Christian, A., Breuer, T., Pajor, N., & Codd, J. R. (2009). Implications of an avian-style respiratory system for gigantism in sauropod dinosaurs. *Journal of Experimental Zoology, Part A: Ecological Genetics and Physiology*, 311, 600–610.
- Prieto-Marquez, A., & Salinas, G. C. (2010). A re-evaluation of *Secernosaurus koernerai* and *Kritosaurus australis* (Dinosauria, Hadrosauridae) from the Late Cretaceous of Argentina. *Journal of Vertebrate Paleontology*, 30, 813–837.
- Prothero, J. (1995). Bone and fat as a function of body weight in adult mammals. *Comparative Biochemistry and Physiology, Part A: Physiology*, 111, 633–639.
- Radermacher, V. J., Fernandez, V., Schachner, E. R., Butler, R. J., Bordy, E. M., Naylor Hudgins, M., de Klerk, W. J., Chapelle, K. E. J., & Choiniere, J. N. (2021). A new *Heterodontosaurus* specimen elucidates the unique ventilatory macroevolution of ornithischian dinosaurs. *eLife*, 10, e66036.
- Rozadilla, S., Brissón-Egli, F., Agnolín, F. L., Aranciaga-Rolando, A. M., & Novas, F. E. (2022). A new hadrosaurid (Dinosauria: Ornithischia) from the Late Cretaceous of northern Patagonia and the radiation of South American hadrosaurids. *Journal of Systematic Palaeontology*, 19, 1207–1235.
- Schachner, E. R., Farmer, C. G., McDonald, A. T., & Dodson, P. (2011). Evolution of the dinosauriform respiratory apparatus: New evidence from the postcranial axial skeleton. *Anatomical Record*, 294, 1532–1547.
- Schachner, E. R., Lyson, T. R., & Dodson, P. (2009). Evolution of the respiratory system in nonavian theropods: Evidence from rib and vertebral morphology. *The Anatomical Record*, 292, 1501–1513.
- Smith, D. K., Sanders, R. K., & Wolfe, D. G. (2021). Vertebral pneumaticity of the North American therizinosaur *Nothronychus*. *Journal of Anatomy*, 238, 598–614.
- Terrill, D. F., Henderson, C. M., & Anderson, J. S. (2020). New application of strontium isotopes reveals evidence of limited migratory behaviour in Late Cretaceous hadrosaurs. *Biology Letters*, 16, 20190930.
- Watanabe, A., Eugenia Leone Gold, M., Brusatte, S. L., Benson, R. B. J., Choiniere, J., Davidson, A., & Norell, M. A. (2015). Vertebral pneumaticity in the ornithomimosaur *Archaeornithomimus* (Dinosauria: Theropoda) revealed by computed tomography imaging and reappraisal of axial pneumaticity in Ornithomimosauria. *PLoS One*, 10, e0145168.
- Wedel, M. J. (2003). Vertebral pneumaticity, air sacs, and the physiology of sauropod dinosaurs. *Paleobiology*, 29, 243–255.
- Wedel, M. J. (2007). What pneumaticity tells us about “prosaupropods”, and vice versa. *Special Papers in Palaeontology*, 77, 207–222.
- Wedel, M. J. (2009). Evidence for bird-like air sacs in saurischian dinosaurs. *Journal of Experimental Zoology. Part A, Ecological Genetics and Physiology*, 311, 611–628.
- Wedel, M. J., Cifelli, R. L., & Sanders, R. K. (2000). Osteology, paleobiology, and relationships of the sauropod dinosaur *Sauroposeidon*. *Acta Palaeontologica Polonica*, 45, 343–388.
- Wedel, M. J., & Taylor, M. P. (2013). Caudal pneumaticity and pneumatic hiatuses in the sauropod dinosaurs *Giraffatitan* and *Apatosaurus*. *PLoS One*, 8, e78213.
- Wilson, J. A. (1999). A nomenclature for vertebral laminae in sauropods and other saurischian dinosaurs. *Journal of Vertebrate Paleontology*, 19, 639–653.
- Wilson, J. A. (2012). New vertebral laminae and patterns of serial variation in vertebral laminae of sauropod dinosaurs. <https://deepblue.lib.umich.edu/bitstream/handle/2027.42/92460/Contributions32no7-HR-c08-15-2012.pdf?sequence=2>
- Wilson, J. A., D'Emic, M. D., Ikejiri, T., Moacdieh, E. M., & Whitlock, J. A. (2011). A nomenclature for vertebral fossae in sauropods and other saurischian dinosaurs. *PLoS One*, 6, e17114.
- Windholz, G. J., Coria, R. A., & Zurriaguz, V. L. (2020). Vertebral pneumatic structures in the Early Cretaceous sauropod dinosaur *Pilmateia faundezi* from northwestern Patagonia, Argentina. *Lethaia*, 53, 369–381.
- Xu, X., Zhao, X., Lü, J., Huang, W., Li, Z., & Dong, Z. (2000). A new iguanodontian from Sangping formation of Neixiang, Henan and its stratigraphical implication. *Vertebrata Palasiatica*, 38, 176–191.
- Yates, A. M., Wedel, M. J., & Bonnan, M. F. (2012). The early evolution of postcranial skeletal pneumaticity in sauropodomorph dinosaurs. *Acta Palaeontologica Polonica*, 57, 85–100.
- Zurriaguz, V. L. (2024). Variation in the postcranial pneumaticity in derived titanosaurs (Dinosauria: Sauropoda). *Historical Biology*, 37, 1–1479.

How to cite this article: Aureliano, T., Ghilardi, A. M., Kaluza, J., & Martinelli, A. G. (2025). Inside a duck-billed dinosaur: Vertebral bone microstructure of *Huallasaurus* (Hadrosauridae), Upper Cretaceous of Patagonia. *The Anatomical Record*, 1–11. <https://doi.org/10.1002/ar.70040>